Rate coefficients for state-to-state rovibronic relaxation in collisions between NO($X\ ^2\Pi$, v=2, Ω, J) and NO, He, and Ar at 295, 200, and 80 K

Meezanul Islam, Ian W. M. Smith, and Jörg W. Wiebrecht
School of Chemistry, The University of Birmingham, Edgbaston, Birmingham B15 2TT, United Kingdom

(Received 18 April 1995; accepted 7 September 1995)

The state-to-state rates of collisional energy transfer within and between the rotational level manifolds associated with the $\Omega=\frac{1}{2}$ and $\Omega=\frac{3}{2}$ spin–orbit states of NO($X\ ^2\Pi$, v=2) have been measured using an infrared–ultraviolet double resonance (IRUVDR) technique. NO molecules were initially prepared in a specific rovibronic level, for example, v=2, $\Omega=\frac{1}{2}$, $J=6.5$, by tuning the output from an optical parametric oscillator (OPO) to a suitable line in the (2,0) overtone band. Laser-induced fluorescence (LIF) spectra of the $A\ ^2\Sigma^+-X\ ^2\Pi$ (2,2) band were then recorded at delay times corresponding to a small fraction of the average time between collisions in the gas sample. From such spectra, the relative concentrations of molecules in levels populated by single collisions from the initially prepared state could be estimated, as could the values of the rate coefficients for the state-to-state processes of collisional energy transfer. Measurements have been made with NO, He, and Ar as the collision partner, and at three temperatures: 295, 200, and 80 K. For all collision partners, the state-to-state rate coefficients decrease with increasing ΔJ (i.e., change in the rotational quantum number and rotational angular momentum) and increasing $\Delta E_{\rm rot}$ (i.e., change in the rotational energy). In NO–NO collisions, there is little propensity for retention of the spin–orbit state of the excited molecule. On the other hand, with He or Ar as the collision partner, transfers within the same spin–orbit state are quite strongly preferred. For transfers between spin–orbit states induced by all collision partners, a propensity to retain the same rotational state was observed, despite the large change in internal energy due to the spin–orbit splitting of 121 cm^{-1}. The results are compared with previous experimental data on rotational energy transfer, for both NO and other molecules, and with the results of theoretical studies. Our results are also discussed in the light of the continuing debate about whether retention of angular momentum or of internal energy is the dominant influence in determining the rates of state-to-state rotational energy transfer.

I. INTRODUCTION

Early experiments on rotational energy transfer—that is, the transfer of molecules between specific rotational states in molecular collisions—were mainly performed on electronically excited states of diatomic molecules. In these experiments, excitation to a specific rovibronic level of the molecule under investigation was achieved using a light source operating continuously in time, which could either be tuned or which contained frequencies that coincided with absorption frequencies in the electronic band system of the molecule. The molecular fluorescence was dispersed and recorded with different pressures of the pure gas or gas mixture present in the sample, and rate coefficients were determined from the relative intensities of the lines in the fluorescent spectrum using the mean radiative lifetime of the electronically excited state as an ''internal clock.'' The experiments of Klemperer and Steinfeld[1] on energy transfer within the $B\ ^3\Pi_{0u^+}$ state of I_2 serve as a classic example of such experiments, the results of which have been reviewed several times,[2,3] some emphasis being placed on the fitting of the experimental data to ''energy gap laws'' within a framework provided by approximate theoretical treatments such as those provided by the infinite-order sudden approximation (IOSA) and energy-corrected sudden (ECS) approximation.

In more recent years, powerful double resonance techniques have been developed to probe the details of collisionally induced energy transfer within the electronic ground state of small molecules. These methods reach their apotheosis when two pulsed tunable laser sources are employed: one to excite molecules in an electric-dipole or Raman allowed transition to a previously unpopulated rovibrational state, the order to observe the evolution of this excited population as collisions occur. The probing is normally achieved by laser-induced fluorescence (LIF) or, less frequently, resonance-enhanced multiphoton ionization (REMPI) techniques using a tunable dye laser. In a number of studies, excitation to rovibrational levels both in homonuclear diatomic molecules like N_2[4] and H_2[5] and in vibrational levels in polyatomic molecules, such as ν_2 in C_2H_2,[6,7] which are not connected to the ground vibrational level by an infrared electric-dipole transition, has been achieved by stimulated Raman excitation. In others, excitation has been the result of direct absorption in fundamental or overtone vibrational bands. Specific levels in NO[8–10] as well as in, for example, C_2H_2[11,12] have been excited in this way for studies of rotational energy transfer. In an important and powerful variant of the double resonance technique, molecules can be excited to high-lying rovibrational levels in their electronic ground state via levels in an electronically excited state through stimulated emission pumping (SEP). Xang and Wodtke[13] have used the SEP

method to study rotational energy transfer within the vibrational levels $\nu=8$ and 19 of NO($X\ ^2\Pi$).

The molecule NO provides a heaven-sent opportunity to examine many of the fine details of collisional energy transfer. On the practical side, it is an infrared-active molecule, so it can be pumped directly to selected excited energy levels in the electronic ground state by tuning laser radiation to transitions in its fundamental or overtone bands. Furthermore, it is easy to observe populations in specific rovibrational levels of NO($X\ ^2\Pi$) using LIF or REMPI via levels in the $A\ ^2\Sigma^+$ or another excited electronic state. On the fundamental side, since NO has a $^2\Pi$ electronic ground state, investigations of energy transfer within this state can examine the details of transfer between spin-orbit states and between the λ-doublet components of individual rotational levels, as well as rotational and vibrational energy transfer.

Inelastic collisions involving NO have previously been the subject of theoretical calculations[14] and molecular beam experiments,[15–17] as well as gas-cell experiments[9] similar to those reported in the present paper. Sudbo and Loy[9] were the first to measure state-to-state rate coefficients for transfer between specific rovibrational levels in NO($X\ ^2\Pi$) in gas-cell experiments. They used a pulsed, tunable, F-center laser to excite NO in its first vibrational overtone band and hence populate individual rotational levels in the $\nu=2$, $\Omega=\frac{3}{2}$ or $\nu=2$, $\Omega=\frac{1}{2}$ spin–orbit level. A dye laser was used to observe the transfer of population from the initially excited state via (1+1) REMPI measurements. As the same laser was used to pump both the infrared and ultraviolet sources, all measurements had to be made at a fixed time delay and the collision time was varied by changing the pressure in the gas sample. Rotational energy transfer induced in collisions with NO, He, Ar, N_2, CO, and SF_6 was investigated at room temperature. Xang and Wodtke,[13] whose experimental technique was mentioned earlier, only investigated energy transfer in NO–NO collisions at room temperature.

Rotational energy transfer in inelastic collisions of NO has also been investigated in three sets of crossed molecular beam experiments.[15–17] Although such experiments are capable of providing information of exquisite detail, in particular differential inelastic cross sections and how the integral and differential cross sections depend on collision energy, they do have some limitations compared with gas-cell experiments. Most importantly, the states prior to any collision are selected only by the supersonic expansion which takes place in the formation of the molecular beam. The large majority of molecules are thereby placed in the ($\nu=0$, $\Omega=\frac{1}{2}$, $J=0.5$) lowest vibronic level and consequently one only obtains values of the cross sections for collisional transfer from this single level.

The first beam studies involving collisions of NO($\nu=0$, $\Omega=\frac{1}{2}$, $J=0.5$), with NO, Ar, and He at a collision energy corresponding to ca. 400 cm^{-1}, were carried out by Joswig *et al.*[15] They used LIF to observe the states of the products of collisions and determined state-to-state integral cross sections. Similar experiments were performed by Jons *et al.*[16] at a slightly higher collision energy ($\equiv$442 cm^{-1}). However, they concentrated on finding differential cross sections by making their LIF measurement, not in the region where the beams crossed, but in a side vessel attached to the main scattering chamber. Finally, Bontuyan *et al.*[17] have measured the inelastic scattering of NO($\nu=0$, $\Omega=\frac{1}{2}$, $J=0.5$) in collisions with Ar using a direct ion imaging technique. As in Sudbo and Loy's experiments,[9] NO in specific product states was ionised by a (1+1) REMPI process through the $A\ ^2\Sigma^+$ state. However, in these experiments, the ions were extracted by an electric field and imaged on a phosphor screen. From an analysis of the resulting image, differential scattering cross sections were calculated for the chosen collision energy corresponding to 1450 cm^{-1}.

The early beam experiments of Joswig *et al.*[15] stimulated detailed theoretical work on NO–Ar collisions by Orlikowski and Alexander.[14(a)] They performed full quantal scattering calculations at 442 cm^{-1} on the potential energy surface calculated by Nielson *et al.*[18] using the electron gas model. Orlikowski and Alexander showed that two potential energy surfaces ($A'+A''$) were important in NO–Ar collisions and that the collisions in which the NO spin–orbit state was preserved took place on an average of the two potentials, whereas spin–orbit changing collisions took place on the difference potential. The centrifugal sudden (CS) approximation was used to simplify the calculation and the number of channels included in the calculation was varied until the results converged. Integral inelastic cross sections were obtained for both spin–orbit conserving and spin–orbit changing transitions.

Following more recent experiments, Alexander[14(c)] carried out new calculations on NO–Ar collisions using a more accurate potential energy surface. The new *ab initio* surface, based on the correlated electron pair approximation (CEPA), gave a better representation of the repulsion between NO and Ar, than the earlier surface which had used the electron gas model. Differential and integral inelastic cross sections were calculated at collision energies corresponding to 442, 149, and 119 cm^{-1}, reflecting the wider range of beam data available by the time these calculations were performed. The experimental and theoretical results were in generally good agreement. In particular, the preference for the integral cross sections to show some oscillation with ΔJ, with even changes being preferred over odd changes, was observed in both the experiments and calculations; an effect which was ascribed to the near homonuclear character of the NO molecule.

In the present paper, we describe the results of state-to-state experiments on rotational energy transfer in NO ($X\ ^2\Pi$, $\nu=2$). Experiments have been performed at three temperatures, 295, 200, and 80 K, with three collision partners, NO, He, and Ar, and on two initial rotational states, $J=0.5$ and 6.5. The principle of our experiments is illustrated in Fig. 1. A subset of NO molecules is excited to a specific rovibronic level using a pulse of tunable infrared radiation from an optical parametric oscillator (OPO-PUMP). The density of these molecules as collisions occur is followed using tunable radiation from a frequency-doubled dye laser (uv-PROBE) to

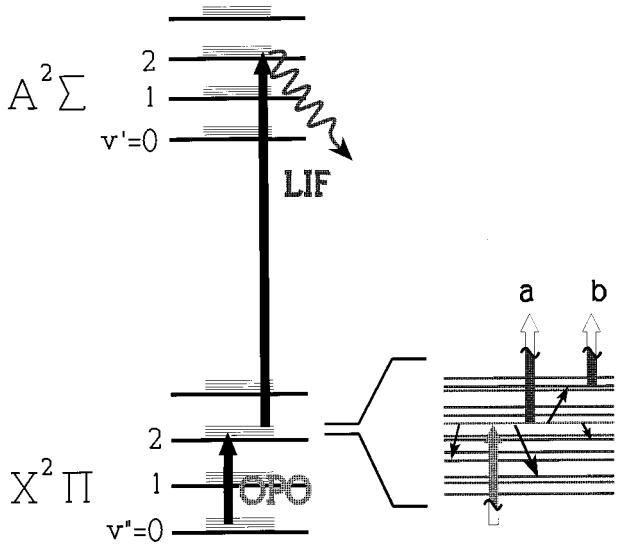

FIG. 1. Infrared–ultraviolet double resonance (IRUVDR) scheme used for energy transfer measurements on NO. The total removal rate from the initially populated level is monitored by observing the LIF signal (a) when the uv-PROBE laser is tuned to a transition out of the level populated by absorption from the OPO-PUMP. Tuning the uv-PROBE to transitions from neighboring levels (b) enables state-to-state rate coefficients to be measured.

excite LIF. As well as recording LIF spectra of the $A\ ^2\Sigma^+ - X\ ^2\Pi$ (2,2) band at short delays in order to deduce the initial distribution of final NO states and hence the rate coefficients for state-to-state energy transfer, we have recorded how the populations in levels neighboring the one excited initially vary with time. The latter kinetic data are modeled using a master equation approach. This procedure and the direct observation of rate coefficients for transfer between the same levels in opposite directions provides information about the propensity (or lack of it) to preserve m_J in rotationally inelastic collisions. In addition, we consider our data in the light of the ongoing controversy[19,20] about whether it is the conservation of angular momentum or of rotational energy which exerts the dominant influence in rotationally inelastic collisions.

II. EXPERIMENT

The experimental arrangement is shown schematically in Fig. 2. NO molecules were excited to selected rovibronic levels using infrared radiation from an optical parametric oscillator, which was pumped by the 1.064 μm output from a Nd:YAG laser which provided pulses of 10–15 ns duration and ca. 100 mJ energy at 10 Hz. To excite molecules to (ν=2, $\Omega=\frac{1}{2}$, J) levels, the frequency of the idler beam from the OPO was tuned into resonance with lines in the P branch of the ($\nu=2\leftarrow0$, $\Omega=\frac{1}{2}\leftarrow\frac{1}{2}$) subband of the first vibrational overtone at ca. 2.7 μm. The pulse energy in the idler beam at this wavelength was in the range 0.1–1.0 mJ, its fluence at the observation zone was 0.5–5.0 mJ cm^{-2}, and its bandwidth was ca. 0.3 cm^{-1}. Fine tuning of the OPO-PUMP output was carried out with the aid of a spectrophone containing 20 Torr of both NO and argon.

The probe radiation was provided by a tunable dye laser (Lambda Physik, FL2002) pumped by an excimer laser (Lumonics, series 400) operated on XeCl. The fundamental output from the dye laser was frequency-doubled in BBO to provide uv-PROBE radiation at 222 nm with a bandwidth of ca. 0.5 cm^{-1}, in order to excite NO electronically in the (2,2) band of the $A\ ^2\Sigma^+ - X\ ^2\Pi$ system. To discriminate against scattered radiation from the probe laser, the fluorescence was observed using a photomultiplier tube (EMI, model 9781B) through a WG 295 broadband filter, which effectively cuts out radiation of wavelengths $<$250 nm.

The bandwidths of both the OPO-PUMP and the uv-PROBE lasers were much greater than the linewidths of the ir and uv transitions in NO. The outputs from both lasers were evidently only weakly polarised (vertically for the OPO

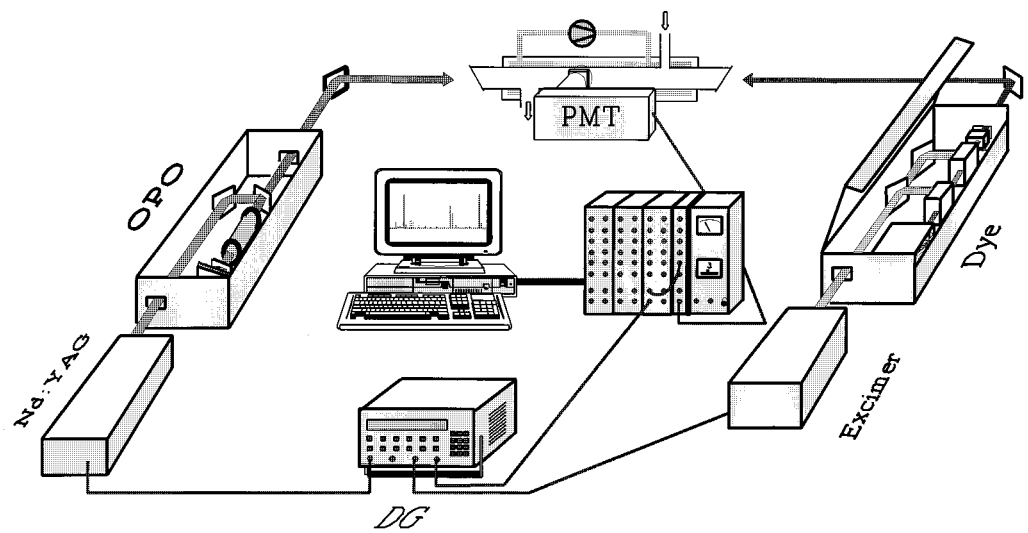

FIG. 2. Schematic of the experimental setup for IRUVDR experiments.

and horizontally for the dye laser) and there is no evidence for significant effects associated with relaxation of m_J, as distinct from J. For example, the derived total relaxation rates seemed independent of a change in the relative polarizations and relative intensities of features in spectra recorded at short delays were consistent with line strength factors based on an assumption of no m_J selectivity.

Use of the cell described by Frost *et al.*[12] allowed experiments to be performed at temperatures down to 80 K. This cell, constructed from Pyrex, has a double jacket, the outer one being permanently evacuated, while refrigerant can be placed in, or passed through, the inner one. To achieve low temperatures, either liquid N_2 was placed in the inner jacket or *iso*-pentane which was cooled in liquid N_2 was circulated through it. The vapor pressure of NO at 80 K is only ca. 100 mTorr but was adequate for the measurements which are reported here.

The beams from the OPO and the dye laser entered and excited the cell through CaF_2 windows mounted at both ends and counterpropagated along its central axis. The fluorescence induced by the dye laser was observed through quartz windows mounted on a short side arm which is joined to the cell at its midpoint and passes through the inner jacket. The photomultiplier, the optical filter and a collecting lens were mounted in a central housing which was clamped to the jacketed cell. The equipment for controlling the firing of the lasers and for recording, accumulating and analysing the LIF signals was the same as that described by Frost and Smith.[12(a)] When recording spectra, LIF signals were normalized to the pulse energies of both the PUMP and PROBE lasers.

The majority of the state-to-state measurements were made following the initial excitation of either the $\nu=2$, $\Omega=\frac{1}{2}$, $J=0.5$ or the $\nu=2$, $\Omega=\frac{1}{2}$, $J=6.5$ level. A smaller number of measurements were made on transfer from other initial levels including $\nu=2$, $\Omega=\frac{3}{2}$, $J=6.5$. The measurements in pure NO were performed with concentrations of between 6×10^{15} and 10×10^{15} molecule cm^{-3}. The experiments designed to study the effects of He and Ar as collision partner were carried out with between 3×10^{15} and 5×10^{15} molecule cm^{-3} of NO and between 2×10^{16} and 5×10^{16} molecule cm^{-3} of He or Ar in the gas sample.

The state-to-state rate coefficients for energy transfer were obtained from LIF spectra recorded with short delays set between the OPO-PUMP and uv-PROBE laser pulses. The delay was chosen to correspond to the time at which $<20\%$ of the excited molecules would have been transferred from the initially excited level. Thus at 295 K and a NO concentration of 7×10^{15} molecule cm^{-3}, a delay of 100 ns was selected; at 80 K, and for NO/Ar mixtures at a total concentration of 4×10^{16} molecule cm^{-3}, a delay of 30 ns was chosen. In order to reduce the effect of jitter in the firing of the two lasers, the intensity at each point in the LIF spectra was the average resulting from ten shots. Principally because of this timing jitter, we estimate 10% errors on the state-to-state rate coefficients for NO–NO collisions and 25% errors on the rate coefficients for NO–He and NO–Ar collisions.

In the kinetics experiments in which time profiles of the LIF signals were recorded, the OPO-PUMP pulse prepared NO in a selected rotational level in ($\nu=2$, $\Omega=\frac{1}{2}$) and the uv-PROBE pulse from the dye laser was tuned to a transition in the $A\ ^2\Sigma^+-X\ ^2\Pi$ (2,2) band emanating from a rovibronic level other than that which was excited directly by the OPO-PUMP. The kinetic behavior of populations in these states was observed by systematically increasing the time delay between the pulses from the PUMP and PROBE lasers keeping the frequencies of both lasers fixed. The delays were synchronized using a pulse generator (Stanford Research Systems, model DG535) and controlled via an IBM-compatible PC via an IEEE interface. In these experiments, the signals at each time delay were averaged over, typically, ten laser shots, but were not normalized to the pulse energies from the OPO-PUMP and uv-PROBE.

At every selected time delay Δt, the signal was averaged over three shots by the boxcar integrator before the time delay was increased. Signals were usually recorded over time delays varied between 100 ns and 3 μs using a stepsize of 30 ns, resulting in 100 points in each scan. To improve the signal:noise on these traces, the results of ten separate scans were averaged before attempting a fit via the master equation approach which is described below.

NO (Electrochem Ltd., 99.99% or Air Products, 99.5%) was admitted to the vacuum line via a liquid N_2 trap and was purified by trap-to-trap distillation until the gas condensed in liquid N_2 as a pure white solid. The sources of the other gases were as follows: He (Air Products, 99.9995%), Ar (BOC, 99.996%). Since the rates of rotational relaxation are so rapid and relatively independent of collision partner, the presence of impurities, even at a level much greater than those quoted, would have a negligible effect on our results.

III. ANALYSIS

A. Determination of state-to-state rate coefficients from PUMP–PROBE experiments at a fixed time delay

At short delays, where there is negligible probability of molecules being transferred back into the initially populated rovibronic level i by collisions, the population of level i ($X\ ^2\Pi$; $\nu=2$; Ω_i; J_i) decays as

$$F_i(t)=N_i(t)/N_i^0=\exp(-k_i n t), \tag{1}$$

where $F_i(t)$ is the fraction of molecules remaining in state i at time t, k_i is the second-order rate coefficient for transfer out of level i, irrespective of final level, and n is the number density of the collision partner. $N_i(t)$ and N_i^0 are the concentrations of NO molecules in the level i at times t and $t=0$. The fraction of the population in a level f populated by single collisions from level i can be expressed as

$$F_f(t)=N_f(t)/N_i^0=(k_{if}/k_i)\{1-\ \exp\ (-k_i n t)\}, \tag{2}$$

where k_{if} is the state-to-state rate coefficient for transfer from level i to level f. At small values of (n,t), i.e., small collision probabilities, this expression simplifies to

$$F_f(t)=(k_{if}/k_i)(k_i n t+\cdots)\approx k_{if} n t \tag{3}$$

with $k_i=\Sigma_f k_{if}$.

Vibrational self-relaxation is ca. 100 times slower than rotational self-relaxation,[10] and the difference is greater for noble gases as collision partners. Consequently, vibrational relaxation can be neglected and the observed depopulation of the initially excited state is mainly caused by rotational energy transfer within the same vibronic manifold, with a smaller contribution (see below) from transfer between the rotational manifolds of the two spin–orbit states. The total rates of depopulation, including loss by diffusion of excited molecules out of the PROBE volume as well as by all forms of collisional energy transfer, could be measured[10] by observing the temporal decay of signals from the level i. The state-to-state rate coefficients, k_{if}, for NO–NO collisions could be determined from experiments on samples of pure NO, by evaluating $F_f(t)$ at a sufficiently short time delay and dividing its value by the product of the time delay and the concentration of NO. The relative intensities of LIF signals from different levels in $X\ ^2\Pi$ could be converted into relative populations using the known rotational line strength factors or by adopting the procedure described in the next paragraph. For mixtures of NO dilute in He or Ar, it was necessary to allow for the effects of NO–NO collisions in order to extract values of k_{if} for NO–He and NO–Ar collisions.

In each experiment designed to yield state-to-state rate coefficients, two LIF spectra were recorded: one at a short time delay corresponding to ca. 15% collision probability, and the other at a much longer time delay, corresponding to ca. 6 collisions and allowing for a Boltzman distribution over rotational states to be established. From these observations, $N_f(t)/N_i^0$ could be calculated in two ways. First, by measuring the intensities of a uv line from the initially populated level at short and long time delays. These intensities could be extrapolated back to $t=0$ to find the initial intensity of the same line. Applying corrections for the relative line strength factors yielded values of $N_f(t)/N_i^0$. Alternatively, N_i^0 could be estimated by summing the intensities of all lines in the rotationally relaxed spectrum. In practice, it was found that the first method led to larger errors, as the large difference in the intensities of lines from the initially populated and other levels in the spectrum recorded at short delays resulted in the signals from level i overloading the boxcar integrator.

The analysis in this part of our investigation was greatly aided by writing a Quick-BASIC program, which allowed LIF spectra to be assigned on screen and which calculated values of $N_f(t)/N_i^0$ and k_{if} automatically.

B. Modeling the profiles of LIF signals with time using a master equation approach

A second way to determine state-to-state rate coefficients for energy transfer within the same vibrational level is to adopt a master equation approach which models the evolution of individual level populations as molecules are transferred among a set of rotational levels. If **N** is the array of level populations and **K** is the matrix of state-to-state rate coefficients for processes connecting the individual levels, the time dependence of **N** is given by

$$\frac{d\mathbf{N}}{dt}=\mathbf{KN}. \tag{4}$$

The complete matrix of state-to-state rate coefficients **K** can be obtained by modeling the time dependence of the populations in the initially excited level and in the levels to which transfer occurs. This kinetic behavior can be calculated by integrating the coupled differential equations which can be written as

$$\frac{dN_j}{dt}=\sum_{k\neq j}\ (k_{kj}N_k+k_jN_j), \tag{5}$$

where k_{kj} is the rate constant for population transfer from level k to level j, k_j is the rate coefficient for total transfer from level j, and N_k, N_j are the populations in levels k, j. In order to reduce the number of differential equations, the model is simplified by including only the lowest 20 rotational levels of each spin–orbit component of $\nu=2$. These levels account for $>96\%$ of a Boltzmann rotational distribution at room temperature, and $>99\%$ for $T=200$ K, and the number of differential equations are reduced to 40. In practice, to model the variation of populations properly at long times, allowance had to be made for loss of population from every level by vibrational relaxation and by diffusion of excited molecules out of the PROBE volume. This was done by including a **j** independent first-order loss term on the right-hand side of each rate equation.

IV. RESULTS

A. Collisionally induced rotational population transfer

The study of the total rates of rotational relaxation from selected rovibronic levels in the electronic ground state of NO($X\ ^2\Pi$), with a variety of collision partners and at three different temperatures from room temperature down to 80 K, has resulted in an extensive body of data which has been published earlier.[10] The total rates of loss from a single rovibronic level were measured by fixing the frequency of the PROBE to coincide with an ultraviolet transition from the initially excited level and scanning the time delay between OPO-PUMP and the uv-PROBE. The rate coefficients for overall relaxation measured by Islam *et al.*[10] (see Tables 1 and 2 of Ref. 10) are essentially independent of the initial rotational and vibrational level of NO, within the ranges covered in those experiments. Furthermore, for most of the collision partners studied, the thermally averaged cross sections for total transfer were found to be independent of temperature within experimental error. There is a slight dependence on collision partner, the cross section being smallest for the light gases, He and H_2, and largest for the molecular collision partners like NO and N_2. Because the second-order rate coefficients for rotational relaxation within the $\nu=2$ and $\nu=3$ levels of NO are very similar, it is reasonable to assume that the state-to-state mechanism for rotational relaxation within different vibrational levels is identical. For this reason, and because measurements on NO($\nu=2$) can be made more accurately, state-to-state rate coefficients have only been measured for NO($\nu=2$).

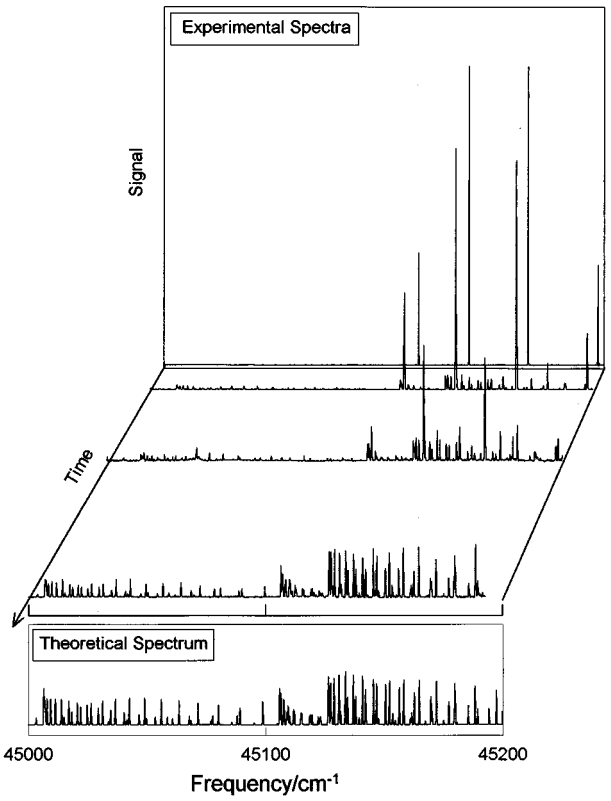

FIG. 3. LIF spectra of the $A\ ^2\Sigma^+ - X\ ^2\Pi$ (2,2) band recorded at different delay times after excitation of 200 mTorr of NO at 295 K to the rovibronic level $X\ ^2\Pi$, $\nu=2$, $\Omega=\frac{1}{2}$, $J=6.5$. The longest time delay is 1 μs, corresponding to ca. 2.5 collisions on average, but the time axis is only approximately linear for the sake of clarity. The theoretical spectrum illustrates the expected appearance of this band from a thermally equilibrated sample at 295 K.

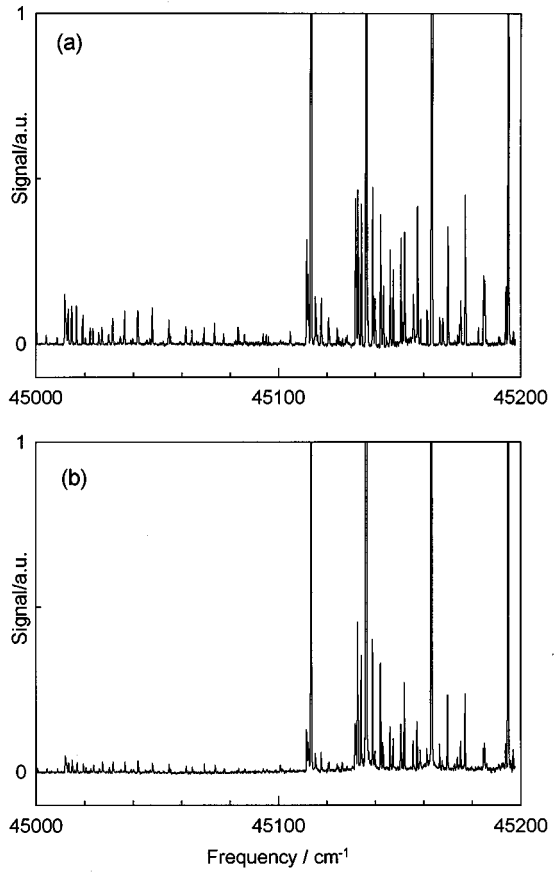

FIG. 4. LIF spectra of the $A\ ^2\Sigma^+ - X\ ^2\Pi$ (2,2) band recorded at 295 K and a delay time of 30 ns corresponding to a collision probability of $P_{\text{coll}} \approx 0.1$ following excitation of (a) 300 mTorr of pure NO, and (b) 60 mTorr of NO diluted to 300 mTorr in Ar, to the rovibronic level $X\ ^2\Pi$, $\nu=2$, $\Omega=\frac{1}{2}$, $J=6.5$.

Rotational state-to-state rate coefficients have been measured in the present work at 295, 200, and 80 K with NO, He, and Ar as collision partners. Most experiments were performed by initially exciting NO to either $\nu=2$, $\Omega=\frac{1}{2}$, $J=0.5$ or to $\nu=2$, $\Omega=\frac{1}{2}$, $J=6.5$. A smaller number of measurements were carried out with initial excitation to $\nu=2$, $\Omega=\frac{1}{2}$, $J=1.5$ or 4.5 and to $\nu=2$, $\Omega=\frac{3}{2}$, $J=6.5$.

As Fig. 3 shows, under collision-free conditions, the uv-PROBE spectrum is particularly simple consisting of only four lines from the single level populated by the OPO-PROBE. As the time delay between OPO-PUMP and uv-PROBE is increased, the intensities of these lines decrease and lines from other levels in $X\ ^2\Pi$, $\nu=2$ grow stronger. The observed frequencies agree very well with those of the simulated spectrum, calculated with the molecular constants from Ref. 21. The relative line intensities at 1 μs show some differences from those in the calculated spectrum, partly due to the variations in the intensity of the probe laser over the range required to scan the LIF spectrum and because more than 2.5 collisions are required to *fully* establish thermal equilibrium over the rotational and spin–orbit states.

Since there are four allowed uv transitions from each rovibronic state in $X\ ^2\Pi$, the relative population in any single rovibronic level can, in principle, be estimated from the average of four observations. In practice, overlap of spectroscopic lines, the overall quality of the spectrum, and the linewidth of the probe laser meant that this ideal situation applied to only a few rovibronic states. Nevertheless, the relative populations in different levels could generally be calculated from more than one line intensity compensating, to some extent, for fluctuations in the power of the probe laser.

Figure 4 shows typical LIF spectra recorded at a short time delay. In both cases, the initially pumped level was $\nu=2$, $\Omega=\frac{1}{2}$, $J=6.5$ and the temperature was 295 K. The upper spectrum was recorded with a delay time and a pressure of NO which yields a collision probability $P_{\text{coll}} \approx 0.1$. As well as the four strong lines from the initially populated level, the spectrum shows about 80 weaker lines arising from other rotational levels of NO($\nu=2$). The lines to the right-hand side of the diagram, with wave numbers $>45\,110$ cm^{-1} correspond to transitions from the lower ($\Omega=\frac{1}{2}$) spin–orbit component, whilst those with frequencies $<45\,110$ cm^{-1} arise from the upper ($\Omega=\frac{3}{2}$) spin–orbit component. This probe spectrum, and others like it, show that molecules are transferred in single collisions to many different rotational levels, up to and including $J=15.5$.

State-to-state rate coefficients for each observed relaxation channel have been calculated by the method described

TABLE I. State-to-state rate coefficients for rotational energy transfer from different initial levels in spin–orbit preserving and spin–orbit changing collisions between NO ($v=2$, Ω, J) and NO at 295 and 200 K. The asterisks (*) denote the initially populated rovibronic levels.

J_{final}	Ω_{final}	$k_{\text{st.-to-st.}}/(\mu\text{Torr}^{-1}\,\text{s}^{-1})$ $T=295$ K	$k_{\text{st.-to-st.}}/(\mu\text{Torr}^{-1}\,\text{s}^{-1})$ $T=295$ K	$k_{\text{st.-to-st.}}/(\mu\text{Torr}^{-1}\,\text{s}^{-1})$ $T=295$ K	$k_{\text{st.-t-st.}}/(\mu\text{Torr}^{-1}\,\text{s}^{-1})$ $T=200$ K	$k_{\text{st.-to-st.}}/(\mu\text{Torr}^{-1}\,\text{s}^{-1})$ $T=200$ K	$k_{\text{st.-to.st.}}/(\mu\text{Torr}^{-1}\,\text{s}^{-1})$ $T=200$ K
0.5	0.5	*	0.15	0.11	*	0.25	0.28
1.5	0.5	1.58	0.44	0.18	3.36	0.48	0.68
2.5	0.5	1.64	0.57	0.50	1.69	0.85	0.61
3.5	0.5	0.87	0.69	0.53	1.44	0.91	0.74
4.5	0.5	1.34	1.21	0.64	1.30	1.73	0.78
5.5	0.5	1.04	1.26	1.05	0.77	1.63	1.11
6.5	0.5	0.91	*	1.15	0.70	*	1.48
7.5	0.5	0.53	1.23	0.74	0.40	1.23	1.17
8.5	0.5	0.67	1.23	0.74	0.40	1.21	0.79
9.5	0.5	0.34	0.71	0.69		0.72	0.53
10.5	0.5		0.72	0.79	0.56	0.74	0.57
11.5	0.5		0.41	0.23		0.25	
12.5	0.5	0.26	0.27	0.27		0.33	0.33
13.5	0.5		0.20	0.19		0.14	
14.5	0.5		0.15	0.19			
15.5	0.5		0.12	0.10			
1.5	1.5		0.09	0.20	0.63	0.18	0.20
2.5	1.5		0.17	0.22	0.43	0.30	0.27
3.5	1.5		0.18	0.48	0.34	0.37	0.45
4.5	1.5		0.24	0.72	0.34	0.48	0.62
5.5	1.5		0.33	0.91	0.27	0.56	0.67
6.5	1.5		0.40	*	0.30	0.58	*
7.5	1.5		0.37	0.78		0.43	0.51
8.5	1.5		0.24	0.71		0.30	0.41
9.5	1.5		0.15	0.37		0.21	0.27
10.5	1.5		0.12	0.24		0.16	0.18
11.5	1.5		0.09	0.17		0.09	
12.5	1.5		0.07	0.16			
13.5	1.5		0.06	0.12			
14.5	1.5		0.04				
15.5	1.5		0.03				
16.5	1.5		0.02				
17.5	1.5		0.03				
	$\Sigma\, k_{ij}=$	9.2±0.2	12.1±0.3	13.2±0.3	12.9±0.1	14.6±0.3	12.7±1.9
	$k_{2\text{nd}}=$	11.6±0.1	12.3±0.3	12.0±0.3	12.8±0.2	14.3±0.1	14.7±1.3

in Sec. III. The results are listed in Tables I–IV. In Fig. 5(a), the state-to-state rate coefficients for transfer from $\nu=2$, $\Omega=\frac{1}{2}$, $J=6.5$ at $T=295$ K and with NO as collision partner are shown as a function of final rotational state. Those for small changes in rotational angular momentum, i.e., small ΔJ, are larger than those for large ΔJ for both Ω preserving and Ω changing transitions. The rate coefficients for transfer to rotational levels of the spin–orbit manifold different from that containing the initially excited level are consistent with an exponential gap law (see below). However, for transfers within the same spin–orbit component, the rate coefficients do not decrease monotonically with ΔJ or change in internal energy ΔE, rather there is some preference for even ΔJ rather than odd ΔJ, although this propensity is only just observable, as these even–odd fluctuations are of the same order as the error bars on the values of the individual rate coefficients.

With NO as collision partner and a temperature of 295 K, the rate coefficients for transfer from $\Omega=\frac{1}{2}$ to $\Omega=\frac{3}{2}$ are smaller than the corresponding rate coefficients for transfer within the $\Omega=\frac{1}{2}$ manifold. However, this difference arises, in large part, from the Boltzmann factor, $\exp(-\Delta E_{\text{s-o}}/RT)$, where $\Delta E_{\text{s-o}}$ is the splitting between the two spin–orbit components. In NO–NO collisions there is otherwise no large propensity for retention of Ω, although the situation is clearly different [see Fig. 5(b)] in collisions of NO with Ar and He.

The observed rate of total loss out of the initially populated level should, of course, correspond to the sum of the state-to-state rate coefficients for rotational relaxation, including spin–orbit changes, and vibrational relaxation. Moreover, because rotational relaxation is much faster than vibrational relaxation or diffusion out of the PROBE volume, the total loss rate is almost identical to that of rotational relaxation. At the foot of Tables I and II, we give $\Sigma_f k_{if}$, the sum of the state-to-state rate coefficients for rotational and spin–orbit transfer from $\nu=2$, $\Omega=\frac{1}{2}$, J and k_i the directly observed rate coefficient for total loss out of the same level. For spectra recorded with good signal:noise ratio, like that shown in Fig. 5(a), the two values are the same within ex-

TABLE II. State-to-state rate coefficients for rotational energy transfer from different initial levels in spin–orbit preserving and spin–orbit changing collisions between NO ($v=2$, Ω, J) and NO at 80 K. The asterisks (*) denote the initially populated rovibronic levels.

J_{final}	Ω_{final}	$k_{\text{st.-to-st.}}/(\mu\text{Torr}^{-1}\,\text{s}^{-1})$	$k_{\text{st.-to-st.}}/[\mu\text{Torr}^{-1}\,\text{s}^{-1})$	$k_{\text{st.-to-st.}}/(\mu\text{Torr}^{-1}\,\text{s}^{-1})$	$k_{\text{st.-to-st.}}/(\mu\text{Torr}^{-1}\,\text{s}^{-1})$	$k_{\text{st.-to-st.}}/(\mu\text{Torr}^{-1}\,\text{s}^{-1})$
0.5	0.5	*	3.08	1.35	0.84	3.08
1.5	0.5	5.45	*	2.29	2.32	
2.5	0.5	6.22	6.14	4.19	2.60	6.14
3.5	0.5	4.95	5.32	4.76	3.61	5.33
4.5	0.5	3.77	3.33	*	2.99	3.33
5.5	0.5	2.47	2.10	3.73	3.82	2.10
6.5	0.5	2.20	1.40	1.85	*	1.40
7.5	0.5	1.35	1.62	1.35	3.18	1.62
8.5	0.5	0.72	0.50	1.12	2.19	0.50
9.5	0.5	0.78		0.49	0.80	
10.5	0.5				0.32	
11.5	0.5			0.27	0.20	
12.5	1.5				0.15	
1.5	1.5	0.51	0.27		0.27	2.67
2.5	1.5		0.40		0.27	3.99
3.5	1.5				0.41	
4.5	1.5		0.20		0.46	1.97
5.5	1.5				0.28	
6.5	1.5				0.26	*
7.5	1.5		0.09		0.09	0.89
8.5	1.5					
9.5	1.5				0.14	
10.5	1.5				0.07	
	$\Sigma\, k_{ij}=$	28.4±0.57	25.2±0.33	21.4±0.31	25.4±0.27	25.2±0.37
	$k_{2\text{nd}}=$	26.1±0.24			28.5±0.24	30.0±0.45

TABLE III. State-to-state rate coefficients for rotational energy transfer from different initial levels in spin–orbit preserving and spin–orbit changing collisions of NO ($v=2$, Ω, J) in mixtures containing 20% NO in Ar at 295, 200, and 80 K. The asterisks (*) denote the initially populated rovibronic levels.

J_{final}	Ω_{final}	$k_{\text{st.-to-st.}}/(\mu\text{Torr}^{-1}\,\text{s}^{-1})$ $T=295$ K	$k_{\text{st.-to-st.}}/(\mu\text{Torr}^{-1}\,\text{s}^{-1})$ $T=295$ K	$k_{\text{st.-to-st.}}/(\mu\text{Torr}^{-1}\,\text{s}^{-1})$ $T=200$ K	$k_{\text{st.-to-st.}}/(\mu\text{Torr}^{-1}\,\text{s}^{-1})$ $T=200$ K	$k_{\text{st.-to-st.}}/(\mu\text{Torr}^{-1}\,\text{s}^{-1})$ $T=80$ K	$k_{\text{st.-to-st.}}/(\mu\text{Torr}^{-1}\,\text{s}^{-1})$ $T=80$ K
0.5	0.5	*	0.07	*	0.24	*	0.49
1.5	0.5	1.04	0.16	1.39	0.12	2.93	0.70
2.5	0.5	0.77	0.32	1.12	0.38	3.87	1.38
3.5	0.5	0.34	0.28	0.71	0.57	1.60	1.41
4.5	0.5	0.33	0.62	0.79	1.06	1.72	1.79
5.5	0.5	0.20	0.41	0.40	0.68	1.07	1.88
6.5	0.5	0.20	*	0.45	*	0.81	*
7.5	0.5	0.11	0.52	0.48	0.40	0.27	1.22
8.5	0.5	0.06	0.52		0.86	0.33	0.87
9.5	0.5	0.05	0.23		0.37		0.32
10.5	0.5		0.26		0.21		0.35
11.5	0.5		0.12		0.18		
12.5	0.5		0.11		0.15		
1.5	1.5	0.17	0.03		0.07		0.32
2.5	1.5	0.10	0.04		0.11		0.34
3.5	1.5	0.08	0.05		0.13		0.29
4.5	1.5	0.09	0.06		0.15		0.45
5.5	1.5	0.11	0.07		0.13		0.22
6.5	1.5	0.06	0.09		0.19		0.21
7.5	1.5	0.05	0.07		0.14		0.15
8.5	1.5	0.04	0.06		0.08		
9.5	1.5	0.03	0.04		0.06		
10.5	1.5	0.02	0.03		0.08		
	$\Sigma\, k_{ij}=$	4.0±1.0	4.4±0.9	5.4±1.1	6.45±1.3	5.4±1.1	12.4±2.6
	$k_{2\text{nd}}=$	6.3±1.0	6.2±1.5	8.4±1.4	9.1±1.9	8.4±1.4	16.1±2.4

TABLE IV. State-to-state rate coefficients for rotational energy transfer from different initial levels in spin–orbit preserving and spin–orbit changing collisions of NO ($v=2$, Ω, J) in mixtures containing 20% NO in He at 295, 200, and 80 K. The asterisks (*) denote the initially populated rovibronic levels.

J_{final}	Ω_{final}	$k_{\text{st.-to-st.}}/(\mu\text{Torr}^{-1}\,\text{s}^{-1})$ $T=295$ K	$k_{\text{st.-to-st.}}/(\mu\text{Torr}^{-1}\,\text{s}^{-1})$ $T=295$ K	$k_{\text{st.-to-st.}}/(\mu\text{Torr}^{-1}\,\text{s}^{-1})$ $T=200$ K	$k_{\text{st.-to-st.}}/(\mu\text{Torr}^{-1}\,\text{s}^{-1})$ $T=200$ K	$k_{\text{st.-to-st.}}/(\mu\text{Torr}^{-1}\,\text{s}^{-1})$ $T=80$ K	$k_{\text{st.-to-st.}}/(\mu\text{Torr}^{-1}\,\text{s}^{-1})$ $T=80$ K
0.5	0.5	*		*	0.14	*	0.66
1.5	0.5	1.51	0.11	1.67	0.19	3.05	0.44
2.5	0.5	0.59	0.25	1.44	0.73	2.34	0.66
3.5	0.5	0.58	0.14	1.33	0.52	1.28	1.02
4.5	0.5	0.32	0.61	0.80	1.08	1.54	1.88
5.5	0.5	0.22	0.51	0.42	0.87	0.69	1.84
6.5	0.5	0.25	*	0.36	*	0.37	*
7.5	0.5	0.15	0.80	0.29	0.57	0.23	1.16
8.5	0.5	0.11	0.64	0.18	0.59	0.18	1.14
9.5	0.5	0.08	0.25		0.27	0.06	0.21
10.5	0.5	0.02	0.27		0.21		0.15
11.5	0.5	0.03	0.17		0.16		
12.5	0.5		0.12		0.11		
1.5	1.5		0.04		0.12		0.18
2.5	1.5		0.07		0.21		0.22
3.5	1.5		0.07		0.15		0.22
4.5	1.5		0.07		0.21		0.14
5.5	1.5		0.09		0.19		0.07
6.5	1.5		0.08		0.22		0.05
7.5	1.5		0.07		0.16		0.04
8.5	1.5		0.06		0.11		0.05
9.5	1.5		0.04		0.07		
10.5	1.5		0.04		0.08		
	$\Sigma\, k_{ij}=$	4.8±1.0	4.6±0.9	6.5±1.3	6.6±1.3	9.7±2.0	10.1±2
	$k_{2\text{nd}}=$	7.1±1.0	7.7±1.5	7.8±1.4	10.2±1.9	13.0±2.4	17.7±3.6

perimental error. Table I presents our measured state-to-state rate coefficients for NO–NO collisions, for the initial states $\nu=2$, $\Omega=\frac{1}{2}$, $J=0.5$ and 6.5, and $\nu=2$, $\Omega=\frac{3}{2}$, $J=6.5$ for $T=295$ and 200 K, whereas Table II lists state-to-state rate coefficients for transfer from $\nu=2$, $\Omega=\frac{1}{2}$, $J=0.5$, 1.5, 4.5, and 6.5 and $\nu=2$, $\Omega=\frac{3}{2}$, $J=6.5$ for $T=80$ K.

The state-to-state rate coefficients for rotational relaxation from $\nu=2$, $\Omega=\frac{1}{2}$, $J=6.5$ in NO–NO collisions at these three temperatures are displayed in Fig. 6. At 295 K, the shape of the cusp function, which approximately describes the variation of the rate coefficients with ΔJ, is almost symmetric about the initially populated level and the rate coefficients for excitation (''up-transfers'') are almost the same as for de-excitation (''down-transfers''). As expected, the decrease of the rate coefficients with positive ΔJ becomes steeper as the temperature is lowered. Thus at 80 K, the rates of rotational transfer with $\Delta J>2$ are insignificant compared with the total relaxation rate. This is not the case for higher temperatures. The effect of decreasing energy being available at low temperatures is also visible in the small signals from levels in the upper spin–orbit component at 80 K. At this temperature the Boltzmann factor, $\exp(-\Delta E_{\text{s-o}}/RT)$, is only 0.1 so that upward transfers between the two spin–orbit manifolds necessarily become rather slow.

Tables III and IV list state-to-state rate coefficients for rotational energy transfer in collisions in 20% mixtures of NO in Ar and in He. Many of the features found for rotational energy transfer in NO–NO collisions are reproduced when the collision partner is Ar or He. Again, the rates of rotational energy transfer to different final rotational levels within the same spin–orbit state is consistent with an exponential gap law (in either ΔJ or ΔE, see below). In addition, for small ΔJ, the transfers with even ΔJ are apparently preferred over those with odd ΔJ. Because relaxation within the same spin–orbit component in NO–NO collisions is approximately 50% faster than in NO–Ar or NO–He collisions, the state-to-state rate coefficients listed for the mixtures are approximately 10% greater than those for NO–Ar and NO–He collisions alone.

The main difference between NO and Ar or He as collision partners is clearly the difference in their ability to induce changes in the spin–orbit component. With both He and Ar the rate coefficients for Ω-changing collisions are clearly very much smaller than those for Ω-preserving transfers, as is apparent if the specrtra in Figs. 5(a) and 5(b) are compared. The quality of the probe spectra obtained from NO-noble gas mixtures was poorer than that obtained from pure NO, since smaller concentrations of NO had to be used in the former case. Because of the resulting experimental errors and because the rate coefficients for Ω-changing NO–Ar and NO–He collisions are very small, it is impossible to derive numerical values of these state-to-state rate coefficients. These factors largely explain the larger experimental errors and the apparent difference in the values of $\Sigma_f k_{if}$ and k_i for the NO-noble gas systems.

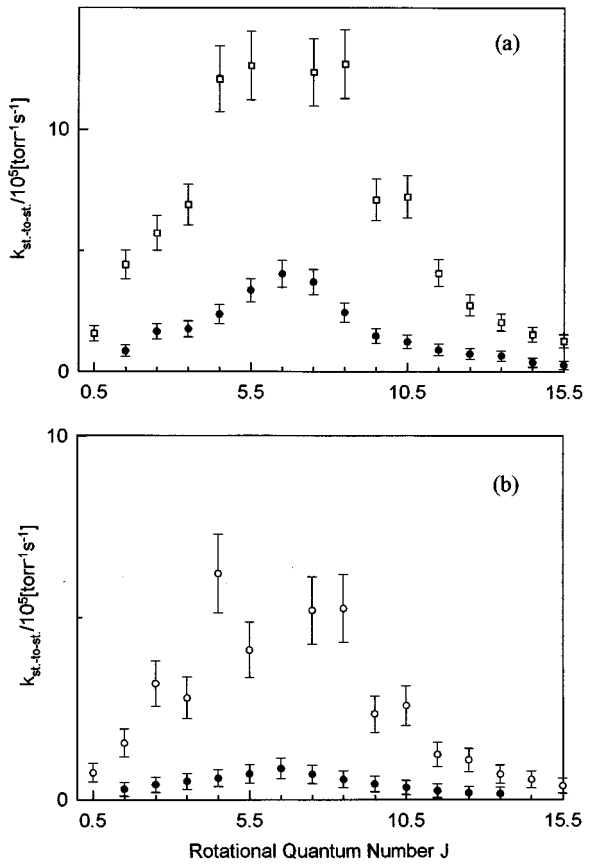

FIG. 5. State-to-state rate coefficients at 295 K for transfer of NO from $v=2$, $\Omega=\frac{1}{2}$, $J=6.5$ in collisions with (a) NO, and (b) in mixtures of 20% NO in Ar. The open circles represent rate coefficients for rotational energy transfer within the same ($\Omega=\frac{1}{2}$) spin–orbit component, and the filled circles those for transfer to levels in the higher ($\Omega=\frac{3}{2}$) spin–orbit component.

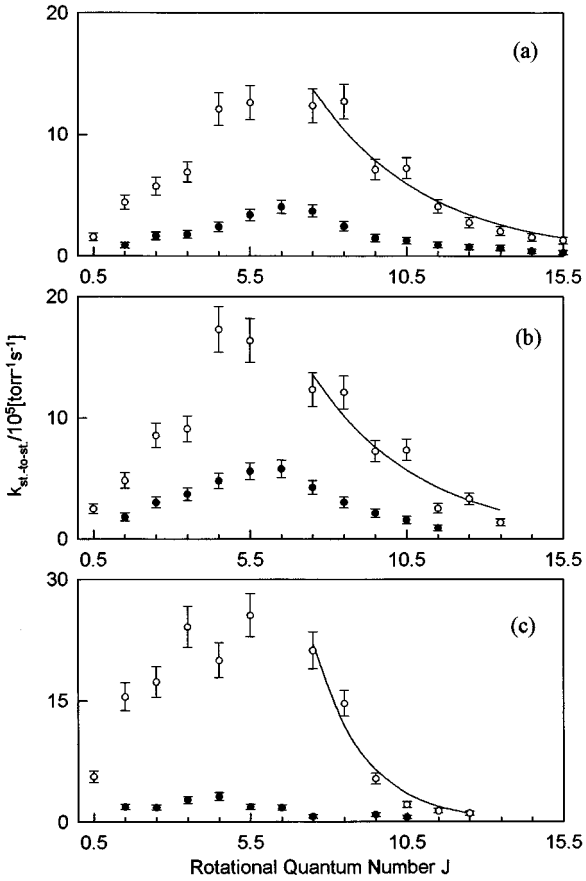

FIG. 6. State-to-state rate coefficients for rotational energy transfer from $v=2$, $\Omega=\frac{1}{2}$, $J=6.5$ in NO–NO collisions at different temperatures: (a) 295 K, (b) 200 K, and (c) 80 K. The lines are fits to the rate coefficients for up transfer to the ΔJ-exponential gap law (see the text).

B. The analysis of state-to-state rotational energy transfer using a master equation approach

For these kinetics experiments the OPO-PUMP was fixed on the $P(7.5)$ transition in the (2,0; $\Omega=\frac{1}{2}\rightarrow\frac{1}{2}$) subband so that NO molecules were initially prepared in the $v=2$, $\Omega=\frac{1}{2}$, $J=6.5$ state. The experiments were carried out at $T=295$ and 200 K. The growth and the decay of population in J levels in $v=2$ were monitored by scanning the PUMP-PROBE delay time with the PROBE frequency fixed to correspond to a uv transition from the particular J level whose kinetics was being observed. Using this method, information concerning collision-induced changes with $\Delta J=\pm1$, ±2, ±3, -4, -5 was collected.

The time dependence of the PROBE signals from several rotational states are displayed in Fig. 7. All these traces show a roughly biexponential variation with time. They mainly differ in their form at small time delays and in their amplitude. The initial rate of increase of the signals from different levels differ. For example, for $J=5.5$ the initial increase is much steeper than for $J=1.5$. At an NO pressure of 300 mTorr and with a time delay $\Delta t=3$ μs, the longest used in these measurements, every molecule has undergone an average of nine collisions and the rotational distribution is totally relaxed. By contrast, if Δt is only 30 ns and $p(\mathrm{NO})=300$ mTorr the collision probability $P_{\mathrm{coll}}\approx0.1$. These conditions are those used to obtain the PROBE spectrum shown in Fig. 4(a) and to derive the state-to-state rate coefficients in the manner described in the previous section.

To first approximation, the LIF signals rise linearly with time at delays which are short enough to correspond to $P_{\mathrm{coll}}<0.2$. In this range, the slope of the signal vs time profile is directly proportional to the state-to-state rate coefficient corresponding to transfer directly from the initially populated level to the level whose population is being observed. As the delay between PUMP and PROBE is increased, the variation of the LIF signals with time becomes less simple, since a significant number of relaxation processes begin to contribute to the time dependence of the observed concentration.

In order to analyze the kinetics of collision-induced rotational energy transfer in NO, we have adopted the master equation model described above. With 40 rotational levels included, the model requires the values of 1600 state-to-state rate coefficients. With only 18 time-dependent PROBE signals available, and each of these carrying significant experimental errors, it was clearly necessary to reduce the number of independent variables before attempting a fit between the experimental results and the simulations. This was done by

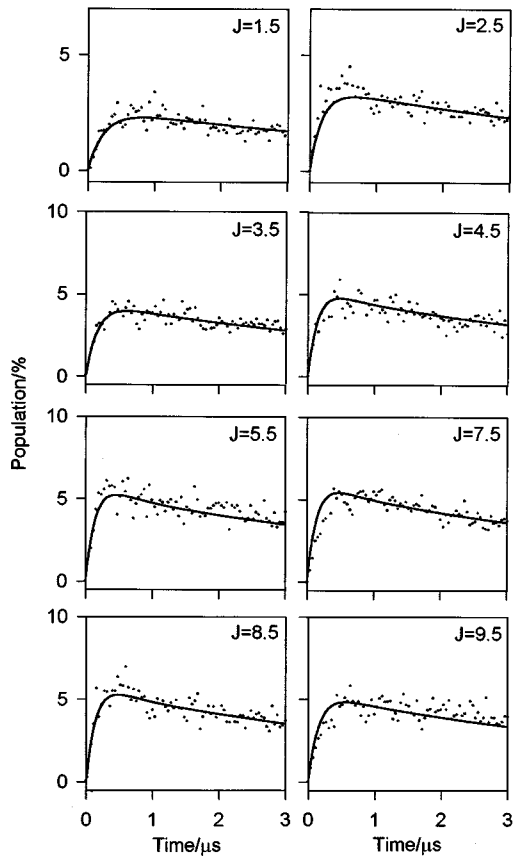

FIG. 7. Kinetic plots showing the variation of individual populations with time following initial excitation of the $\nu=2$, $\Omega=\frac{1}{2}$, $J=6.5$ level in a sample of 300 mTorr pure NO. The points represent the experimental data. The curves are calculated from a model based on the use of master equations and a two-parameter representation $\{k_{if}=B\exp(-\beta\Delta J)\}$ of the state-to-state rate coefficients.

adopting a number of fitting laws to represent the functional dependence of the state-to-state rate coefficients so as to minimize the number of parameters in the kinetic matrix **K**. For transfers within the same spin–orbit component, three different fitting laws have been tested. In two, the values of the state-to-state rate coefficients were assumed to depend on $\Delta E_{\rm rot}$, the difference in rotational energy between the initial and final states; in the third, the state-to-state rate coefficients depend on ΔJ, the difference in rotational momentum between the states. Explicitly, the fitting laws considered for $\Delta\Omega=0$ are as follows:

Exponential energy gap law

$$k_{if}=A\ \exp(-\alpha|\Delta E_{\rm rot}|/k_BT), \tag{6a}$$

Energy power gap law

$$k_{if}=C(|\Delta E_{\rm rot}|/k_BT)^{-\gamma}, \tag{6b}$$

Exponential angular momentum gap law

$$k_{if}=B\ \exp(-\beta|\Delta J|). \tag{6c}$$

Here, k_B is the Boltzmann constant and T the absolute temperature. Each fitting law has two adjustable parameters, A and a for the energy gap fitting law, B and β for the angular momentum gap fitting law, and C and γ for the power gap fitting law. The rate coefficients for exothermic transfers were assumed to obey one of the fitting laws given in Eqs. (6a)–(6c) while those for endothermic transfers were calculated via the principle of detailed balance according to the relationship

$$(k_{if}/k_{fi})=\{(2J_f+1)/(2J_i+1)\}\exp([E_i-E_f]/k_BT). \tag{7}$$

The calculations also assumed that the sum of the state-to-state rate coefficients for rotational energy transfer from a particular level corresponded to the rate of total loss from that level; i.e., $k_i=-\Sigma_{i\neq f}k_{if}$.

Traditionally, the exponential energy gap law for rotational energy transfer has referred to an overall energy deficit $|\Delta E_{RT}|$ for the *pair* of colliding molecules; that is, it has taken into account changes of internal state in *both* molecules. For an atom as the collision partner, there is, of course, a change of internal state only in the observed molecule. On the other hand, for a molecule as collision partner, energy can also be transferred by $R-R$ energy transfer thereby, in principle, reducing the energy mismatch. The possible role of such processes has been investigated for HF–HF collisions.[22] It was concluded that even HF, which is strongly polar and has widely spaced rotational levels, can be treated like an atom-like collision partner, at least in thermally equilibrated samples, and that the exponential energy gap law can be used with the energy difference $|\Delta E_{if}|$ instead of $|\Delta E_{RT}|$. This encouraged us to use this law in analyzing the results of rotational energy transfer in collisions between NO molecules.

The master equation model which has been used to simulate changes in J within NO ($X\ ^2\Pi$, $\nu=2$, $\Omega=\frac{1}{2}$) is very well known, as are the equations used to calculate the detailed balance factor and the energies of the individual states. Kinetic traces predicting the time development of the PROBE intensity have been calculated for each of the proposed fitting laws. The computed curves are compared with the PROBE traces in Fig. 7. The state-to-state rate coefficients for direct transfer to other rotational levels from $\nu=2$, $\Omega=\frac{1}{2}$, $J=6.5$, which was the level initially populated by the OPO-PROBE in the experiments, have been extracted out of the kinetic matrix and are listed in Table V. All the different fitting laws predict very similar state-to-state rate coefficients. The parameters for the simulations using all three fitting laws are given in Table V.

V. DISCUSSION

The only results which can be directly compared with the state-to-state rate coefficients reported in the present paper are those determined by Sudbo and Loy.[15] Their data set is more limited than our own and they made measurements only at room temperature. In addition, their experimental method differed in several significant ways from that employed in the present study. For example, they operated at a fixed, very short, time delay ($\Delta t=30$ ns) and higher sample pressures. In each series of experiments, they fixed the frequency of their uv-PROBE, which generated REMPI signals via lines in the $A\ ^2\Sigma^+-X\ ^2\Pi(2,2)$ band, and scanned the

TABLE V. Comparison of experimental state-to-state rate coefficients for transfer from the $\nu=2$, $\Omega=0.5$, $J=6.5$ level in NO–NO collisions at 295 and 200 K with the values predicted from the kinetic simulations using the three forms of the fitting laws given in the text (e.e.g.l≡exponential energy gap law; e.a.g.l.≡exponential angular momentum gap law; p.g.l.≡power gap law). The parameters used in the fitting laws are given in the last two lines of the table.

J_{final} $\Omega=0.5$	$k_{\text{st.-to-st.}}/(\mu\text{Torr}^{-1}\,\text{s}^{-1})$ $T=295$ K exp. data	$k_{\text{st.-to-st.}}/(\mu\text{Torr}^{-1}\,\text{s}^{-1})$ $T=295$ K e.e.g.l.	$k_{\text{st.-to-st.}}/(\mu\text{Torr}^{-1}\,\text{s}^{-1})$ $T=295$ K e.a.g.l.	$k_{\text{st.-to-st.}}/(\mu\text{Torr}^{-1}\,\text{s}^{-1})$ $T=295$ K p.g.l.	$k_{\text{st.-to-st.}}/(\mu\text{Torr}^{-1}\,\text{s}^{-1})$ $T=200$ K exp. data	$k_{\text{st.-to-st.}}/(\mu\text{Torr}^{-1}\,\text{s}^{-1})$ $T=200$ K e.e.g.l.	$k_{\text{st.-to-st.}}/(\mu\text{Torr}^{-1}\,\text{s}^{-1})$ $T=200$ K e.a.g.l.	$k_{\text{st.-to-st.}}/(\mu\text{Torr}^{-1}\,\text{s}^{-1})$ $T=200$ K p.g.l.
0.5	0.15	0.19	0.29	0.19	0.25	0.23	0.28	0.23
1.5	0.44	0.32	0.35	0.31	0.48	0.39	0.36	0.37
2.5	0.57	0.61	0.61	0.58	0.85	0.76	0.65	0.68
3.5	0.69	0.71	0.71	0.65	0.91	0.90	0.79	0.76
4.5	1.21	1.16	1.19	1.07	1.73	1.53	1.38	1.25
5.5	1.26	1.25	1.34	1.28	1.63	1.72	1.60	1.51
6.5	*	*	*	*	*	*	*	*
7.5	1.23	1.27	1.38	1.26	1.23	1.64	1.56	1.39
8.5	1.23	1.18	1.26	1.08	1.21	1.33	1.33	1.12
9.5	0.71	0.71	0.78	0.71	0.72	0.69	0.76	0.71
10.5	0.72	0.62	0.69	0.74	0.74	0.51	0.63	0.72
11.5	0.41	0.35	0.42	0.53	0.25	0.24	0.36	0.50
12.5	0.27	0.28	0.37	0.58	0.33	0.16	0.29	0.54
13.5	0.20	0.15	0.22	0.43	0.14	0.07	0.16	0.40
14.5	0.15	0.11	0.19	0.48		0.04	0.13	0.44
15.5	0.12	0.06	0.11	0.37		0.02	0.07	0.33
		$\alpha=2$ $A=1.8$	$\beta=0.4$ $B=1.9$	$\gamma=0.47$ $C=0.52$		$\alpha=2$ $A=2.6$	$\beta=0.47$ $B=2.3$	$\gamma=0.55$ $C=0.6$

frequency of the infrared PUMP laser which was a pulsed color-center laser. Thus their experiments naturally generated a set of state-to-state rate coefficients for transfer *into* a particular *final* state rather than a set of state-to-state rate coefficients for transfer *from* a particular *initial* state, as in our experiments.

To facilitate a comparison of these two sets of results, in Table VI we list the total and state-to-state rate coefficients for transfer between rotational levels in NO ($\nu=2$, $\Omega=\frac{1}{2}$) in NO–NO collisions at room temperature determined in both the present work and by Sudbo and Loy.[15] Although there are significant differences between individual values of the state-

TABLE VI. Comparison of state-to-state rate coefficients for transfer within the $\Omega=\frac{1}{2}$ spin–orbit component in NO–NO collisions at 295 K measured in the present work with those measured by Sudbo and Loy [Ref. 15(b)]. The rate coefficients are given in units of $(\mu\text{Torr}^{-1}\,\text{s}^{-1})$. The horizontal lines of numbers marked with an asterisk are taken from Sudbo and Loy [Ref. 15(b)]. The remainder of the rate coefficients are from the present work.

	J_{initial}																		
J_{final}	0.5	1.5	2.5	3.5	4.5	5.5	6.5	7.5	8.5	9.5	10.5	11.5	12.5	13.5	14.5	15.5	16.5	17.5	18.5
0.5	(11.6)						0.15												
*0.5	(13.1)	1.0																	
1.5	1.58						0.44												
*1.5	1.8	(11.6)	0.8	0.8	0.4	0.3													
2.5	1.64						0.57												
*2.5	1.8	1.8	(13.3)	1.5	1.0	0.8													
3.5	0.87						0.69												
4.5	1.34						1.21												
5.5	1.04						1.26												
6.5	0.91						(12.3)												
7.5	0.53						1.23												
8.5	0.67						1.23												
*8.5	0.1	0.3	0.4	0.6	0.5	0.5	0.5	0.9	(10.0)	0.8	1.6	0.6	0.3						
9.5	0.34						0.71												
10.5							0.72												
*10.5										0.7	(10.3)								
11.5							0.41												
12.5	0.26						0.27												
13.5							0.20												
14.5							0.15												
15.5							0.12												
16.5																			
*16.5												0.1	0.1	3	0.8	0.6	(13.8)	1.1	1.9

to-state rate coefficients, it is evident that there is good general agreement between the results of these two investigations. In particular, we agree (i) on the magnitude of the rate coefficients for total removal of population from an initially populated level and that these rate coefficients are essentially independent of J within the range of J levels which are significantly populated at room temperature; and (ii) that the state-to-state rate coefficients show a general decrease as the values of ΔJ (or ΔE_{rot}) increases.

Rate coefficients for rotational energy transfer can also be usefully compared with the parameters characterizing collision broadening of spectroscopic transitions in the same molecule. As pointed out previously,[10] there have been a large number of studies of collision broadening[23] of infrared transitions in NO. Two of the most recent and thorough sets of experiments are those of Pine *et al.*[23(b),23(c)] on lines in the (2,0) first overtone band. Second-order rate coefficients can be calculated from collision-broadening coefficients and compared with those for rotational energy transfer determined in direct experiments. Any discrepancy indicates the existence of collision-broadening mechanisms other than rotational energy transfer. We have noted elsewhere[10] that there is a small but significant discrepancy in the case of NO–NO collisions, with the rate coefficients derived from pressure-broadening data being larger than those measured directly, and have tentatively ascribed this difference to the contribution of collisions which change m_J but leave J unchanged. The lack of any propensity to conserve m_J in collisions involving NO is consistent with both the theoretical predictions of Orlikowski and Alexander[14(b)] and our conclusion (see below) that there is no significant propensity to conserve m_J when collisions induce rotational energy transfer. The NO self-broadening and N_2–broadening parameters also show a small (ca. 10%–15%) decrease from the lowest J values to $J=17.5$, as well as larger (ca. 6%) values for the f symmetry components as compared with the e components. However, both these effects are too small to observe in our IRUVDR experiments without a significant increase in accuracy; in particular, a higher shot-to-shot stability in the OPO-PUMP would be required.

The present experiments are, we believe, the first in which a systematic investigation has been made of the temperature dependence of total and state-to-state rate coefficients for rotational energy transfer, at least at temperatures below room temperature. It will be especially interesting to carry the measurements to still lower temperatures when the rates of these collisional processes are likely to become sensitive to the long-range attractive forces between the collision partners.[24] As we have pointed out before, it appears that the thermally averaged cross sections for total transfer, with the possible exception of those for NO–NO collisions, remain unaffected by temperature, so that the rate coefficients scale approximately as $T^{1/2}$, an assumption which is sometimes made in respect of collision-broadening parameters. The main effect of temperature on the state-to-state rate coefficients for rotational energy transfer is chiefly that determined by energetic considerations: the rate coefficients for up transfers, both to rotational levels in the same spin–orbit component and to levels in the higher spin–orbit component, are reduced as the temperature is lowered. This effect is shown for NO–NO collisions in Fig. 6.

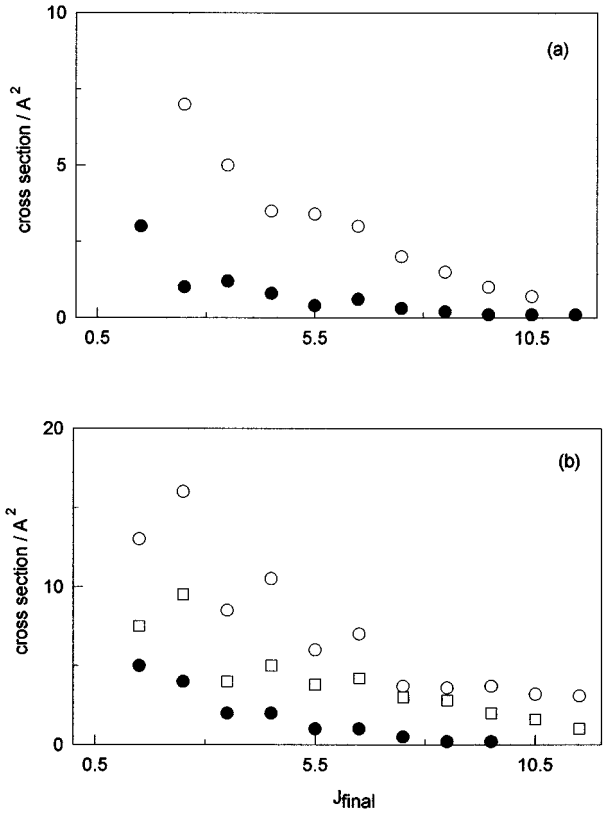

FIG. 8. Comparison of cross sections for transfer from $\nu=2$, $\Omega=\frac{1}{2}$, $J=6.5$ to different final rotational levels within the same spin–orbit component: (a) in NO–He collisions, ●—our thermal experiments at 295 K, ○—the beam experiments of Joswig *et al.* [Ref. 15(b)] at a collision energy of 5.3 kJ mol^{-1}; (b) in NO–Ar collisions, ●—our thermal experiments at 295 K, ○—the beam experiments of Joswig *et al.* [Ref. 15(b)], and □—calculations of Alexander [Ref. 14(c)], both at a collision energy of 6.1 kJ mol^{-1}.

Given the minimal dependence of cross sections for energy transfer on temperature, and therefore presumably on collision energy, in collisions between NO and the rare gases, we have compared thermally averaged cross sections from our experiments on NO–He and NO–Ar mixtures, with the results of the crossed beam experiment by Joswig *et al.*[15(b)] The collision energies in their experiments corresponded to 6.1 and 5.3 kJ mol^{-1} for NO–He and NO–Ar, respectively. At 295 K, the average collision energy $(3k_BT/2)$ is 3.7 kJ mol^{-1}. We have calculated thermally averaged state-to-state cross sections for transfers within the $\Omega=1/2$ spin component in NO–He and NO–Ar collisions from the rate coefficients at 295 K listed in Tables III and IV. The results are compared in Fig. 8 with the cross sections derived by Joswig *et al.*[15(b)] It can be seen that the variation of the cross sections with ΔJ are quite similar in both cases. The absolute values of the cross sections, however, differ significantly. It seems likely that this is the result of the notorious difficulty of transforming signals in crossed molecular beams experiments to *absolute* cross sections. The absolute cross sections reported by Joswig *et al.*[15(b)] are based on

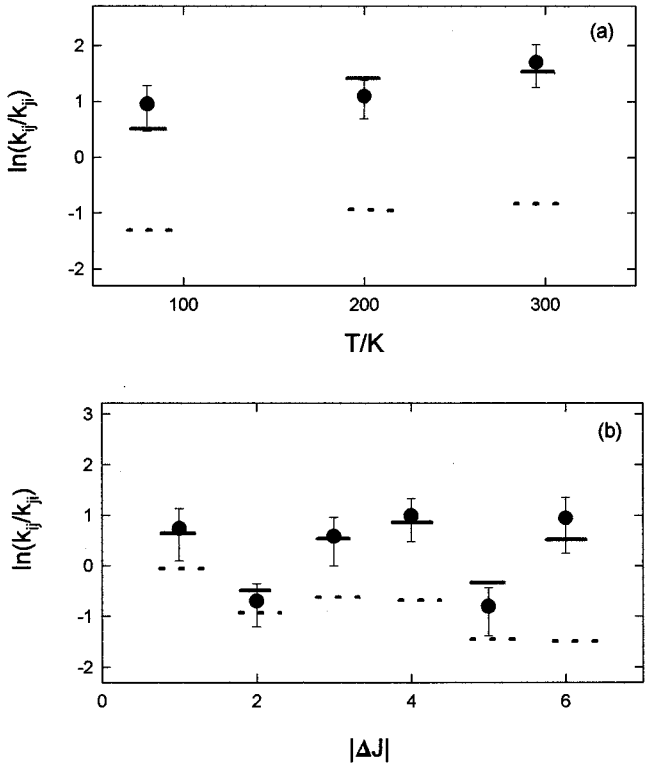

FIG. 9. Comparison of the ratios of state-to-state rate coefficients for forward and reverse transfer with predictions based on detailed balance including (—) and excluding (---) rotational level degeneracies: (a) ratios of rate constants for transfer between $\nu=2$, $\Omega=\frac{1}{2}$, $J=0.5$ and 6.5 at 80, 200, and 295 K; (b) ratios of rate constants for transfer between pairs of levels among $\nu=2$, $\Omega=\frac{1}{2}$, $J=0.5$, 1.5, 4.5, and 6.5 (resulting in six values in total differing in $|\Delta J|$) at 80 K.

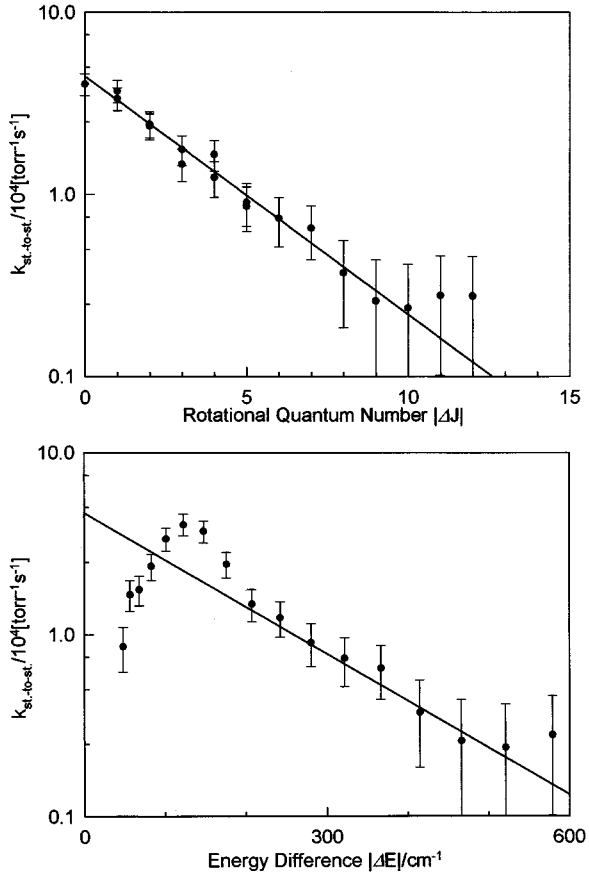

FIG. 10. Test of energy gap, $|\Delta E|$, and angular momentum gap, $|\Delta J|$, representations of the state-to-state rate coefficients for spin–orbit changing processes from $\nu=2$, $\Omega=\frac{1}{2}$, $J=6.5$ to $\nu=2$, $\Omega=\frac{3}{2}$, J at 295 K.

a measurement of the attenuation of the primary NO-containing beam by the secondary, noble gas, beam, and Joswig *et al.* themselves point out that this ''allows a rough estimate of the absolute value of the inelastic cross-sections.'' We note that Alexander,[14(c)] in order to obtain agreement between the results of his quantum scattering calculations based on a corrected electron pair approximation (CEPA) surface to describe the NO–Ar interaction and the experimental results, multiplied the absolute state-to-state cross sections of Joswig *et al.*[15(b)] by a factor of 0.5342. Alexander's results are included on Fig. 8.

It can be seen from Fig. 8 that not only the general decrease in state-to-state rate cross sections with increasing $|\Delta J|$ but also the slight fluctuations between their values for ΔJ even and ΔJ odd for small ΔJ are seen in all three sets of results. Alexander's calculations indicate that these fluctuations would be much greater if state-to-state rate coefficients could be determined which were selective not only in J but also in the λ component of the initial and final state.

Our measurements indicate that at 295 K, the integrated rate coefficient for Ω-changing transfers by He and Ar are no more than 10% of those for Ω-preserving transfers in both cases. These results are in good agreement with those obtained by Joswig *et al.*[15(b)] and the predictions of Alexander.[14(c)] Joswig *et al.* observed, in agreement with Alexander's calculations, that for multipet-changing transfers in collisions between NO($\Omega=\frac{1}{2}$, $J=0.5$) and Ar there is a propensity for quite large changes in J with the cross sections being rather similar for values of ΔJ between 1 and 9.

Orlikowski and Alexander[14(a)] have considered the m_J-preserving propensities in rotationally inelastic collisions involving NO. Although propensities were found for specifically e/f-changing and e/f-preserving collision, they concluded that little propensity would be found in state-to-state cross sections of the type measured in the present experiments. This prediction can be tested by comparing the values of the state-to-state coefficients for transfer between the same two rotational levels but in opposite directions.

Figure 9 displays the results of such a comparison. Panel (a) compares the ratio of the rate coefficients for transfer from state $|i\rangle=(\nu=2,\ \Omega=\frac{1}{2},\ J=0.5)$ to state $|f\rangle=(\nu=2,\ \Omega=\frac{1}{2},\ J=6.5)$ with those for transfer in the opposite direction at 80, 200, and 295 K. Panel (b) makes a similar comparison for transfer in both directions between the states $\nu=2$, $\Omega=\frac{1}{2}$, $J=0.5$, 1.5, 4.5 and 6.5 at 295 K. Both comparisons are clearly consistent with the supposition that there is no propensity for preserving m_J in rotationally inelastic collision, in agreement with the theoretical prediction of Orlikowski and Alexander,[14(a)] and with the supposition that our experiments only probe the results of J-changing transfers. Consequently, the ratio of rate coefficients obeys detailed balance

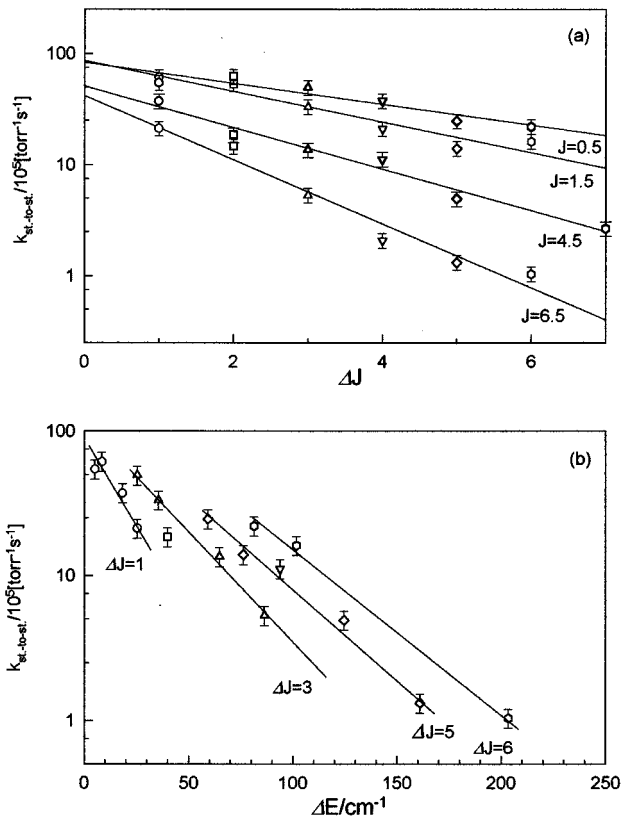

FIG. 11. Spin–orbit conserving state-to-state rate coefficients for rotational energy transfer from four different initial rotational levels: $v=2$, $\Omega=\frac{1}{2}$, $J=0.5$, 1.5, 4.5, 6.5. Graph (a) shows (a) the ΔJ dependence, and (b) the ΔE dependence of the rate coefficients.

according to Eq. (7), as assumed in the master equation calculations used to model the observed kinetic behaviour of individual level populations.

Finally, we consider our results in the light of the continuing debate as to whether changes in internal or rotational energy, $|\Delta E|$, or rotational momentum, $|\Delta J|$, exert a more powerful influence on state-to-state cross sections or rate constants for rotational energy transfer. In general, of course, the changes in $|\Delta E|$ and $|\Delta J|$ are strongly linked so that correlations with either quantity prove satisfactory, whichever is exerting the physical control. Until recently, correlations with $|\Delta E|$ were more common, invoking the IOSA and ECS results as justification. Lately, McCaffery *et al.*[19] and Marks[24] have argued strongly that collisionally induced rotational energy transfer is controlled by the interchange of orbital and rotational momentum which occurs when the collision partners impact on one another.

One revealing finding from our own work emerges from the measured state-to-state rate coefficients for spin–orbit changing collisions. These data, *inter alia*, are displayed in Fig. 5. The propensity is for retention of the rotational quantum number. The same data for spin–orbit changing collisions are shown in a different way in Fig. 10. Here, the logarithm of the rate coefficients for transfer in NO–NO collisions at 295 K are plotted against the changes in (a) rotational quantum number, and (b) the energy difference between initial and final rovibronic states. On this basis, the first-correlation clearly does better, although it should be remembered that an energy gap correlation would be recovered if $|\Delta E|$ was taken to be the change only in the *rotational* energy. Nevertheless, on balance, it seems as if this evidence supports the notion that angular momentum is the dominating influence in rotational energy transfer.

In addition, in Fig. 11, we follow Dopheide *et al.*[7] in plotting the logarithm of state-to-state rate coefficients against $|\Delta J|$ for spin–orbit preserving NO–NO collisions at 80 K, distinguishing the data for different initial rotational levels. Each set of data from a particular initial J level shows a good correlation with ΔJ but the slopes of these plots are different. However, all the points can be brought approximately on to the same line when allowance is made for the different ratio of degeneracies in the pairs of initial and final states. In the second panel of Fig. 11, the same data are plotted in a different way; now against ΔE, with sets of data distinguished by their change in J. Each set shows an approximately linear correlation but the slopes are different for different ΔJ. Once again, these correlations seem to point to the importance of angular momentum effects in rotational energy transfer.

VI. SUMMARY

This paper reports the measurement of an extensive set of state-of-state rate coefficients for rotational energy and spin–orbit transfer in NO ($X\ ^2\Pi$, $v=2$). Effects of collision partner (NO, Ar, He) and temperature (295, 200, 80 K) have been examined. The double resonance method employed in the experiments used a tunable optical parametric oscillator to promote NO molecules to a selected rovibronic level and a tunable dye laser to observe the kinetic behavior of the subset of molecules which had been excited. State-to-state rate coefficients were found by observing relative intensities in the LIF spectra at time delays corresponding to a probability of a collision of $<$ca. 0.2. In addition, kinetic experiments were performed in which the changes in concentration in collisionally populated levels were observed as a function of time delay. Simulating these traces via a master equation model yielded state-to-state rate coefficients in satisfactory agreement with those determined in the more direct experiments.

The results demonstrated that in NO–NO collisions there is little propensity to stay in the same spin–orbit component, in contrast to what is observed in NO–Ar and NO–He collisions. For all collision partners, the state-to-state cross sections decreased with increasing ΔJ with some, scarcely detectable, preference for even changes in J at small ΔJ. Finally, we note the propensity for J to be conserved in collisions in which molecules were transferred between spin–orbit components, despite the relatively large energy difference (ca. 121 cm^{-1}) which this entails. This observation and other evidence incline us to the view that it is the need to transfer angular momentum between orbital motion and molecular rotation, rather than changes in internal energy, which exerts the major influence in determining rates of rotational energy transfer.

ACKNOWLEDGMENTS

We are grateful to SERC for support of this work and the CEC for the award of a Fellowship (J.W.W.) under the Human Capital and Mobility Programme. We also thank Professor F. F. Crim for useful discussions regarding double resonance studies of collisional energy transfer and N.A.T.O. for a Travel Grant to facilitate the cooperation with his laboratory.

[1] J. I. Steinfeld and W. Klemperer, J. Chem. Phys. **42**, 3745 (1965).
[2] T. A. Brunner and D. Pritchard, in *Dynamics of the Excited State*, edited by K. P. Lawley (Wiley, New York, 1982).
[3] A. J. McCaffery, M. J. Proctor, and B. J. Whitaker, Ann. Rev. Phys. Chem. **37**, 223 (1986).
[4] G. O. Sitz and R. L. Farrow, J. Chem. Phys. **93**, 7883 (1990).
[5] (a) D. W. Chandler and R. L. Farrow, J. Chem. Phys. **85**, 810 (1986); (b) R. L. Farrow and D. W. Chandler, *ibid*. **89**, 1994 (1988).
[6] B. L. Chadwick and B. J. Orr, J. Chem. Phys. **97**, 3007 (1992).
[7] (a) R. Dopheide, W. B. Gao, and H. Zacharias, Chem. Phys. Lett. **182**, 21 (1991); (b) R. Dopheide, W. Cronrath, and H. Zacharias, J. Chem. Phys. **101**, 5804 (1994).
[8] P. Esherick and R. J. M. Anderson, Chem. Phys. Lett. **70**, 621 (1980).
[9] (a) Aa. S. Sudbo and M. M. T. Loy, Chem. Phys. Lett. **82**, 135 (1981); (b) Aa. S. Sudbo and M. M. T. Loy, J. Chem. Phys. **76**, 3646 (1982).
[10] (a) M. J. Frost, M. Islam, and I. W. M. Smith, Can. J. Chem. **72**, 606 (1994); (b) M. Islam, I. W. M. Smith, and J. W. Wiebrecht, J. Phys. Chem. **98**, 9285 (1994).
[11] (a) E. Carrasquillo, A. L. Utz, and F. F. Crim, J. Chem. Phys. **88**, 5976 (1988); (b) A. L. Utz, J. D. Tobiason, E. Carrasquillo, M. D. Fritz, and F. F. Crim, *ibid*. **97**, 389 (1992); (c) J. D. Tobiason, A. L. Utz, and F. F. Crim, *ibid*. **101**, 1108 (1994).
[12] (a) M. J. Frost and I. W. M. Smith, Chem. Phys. Lett. **191**, 574 (1992); (b) M. J. Frost, J. Chem. Phys. **98**, 8572 (1993).
[13] X. Yang and A. M. Wodtke, J. Chem. Phys. **96**, 5123 (1992).
[14] (a) T. Orlikowski and M. H. Alexander, J. Chem. Phys. **79**, 6006 (1983); (b) T. Orlikowski and M. H. Alexander, *ibid*. **80**, 4133 (1984); (c) M. H. Alexander, *ibid*. **99**, 7725 (1993).
[15] (a) P. Andresen, H. Joswig, H. Pauly, and R. Schinke, J. Chem. Phys. **77**, 2204 (1982); (b) H. Joswig, P. Andresen, and R. Schinke, *ibid*. **85**, 1904 (1986).
[16] S. D. Jons, J. E. Shirley, M. T Vonk, C. F. Giese, and W. R. Gentry, J. Chem. Phys. **97**, 7831 (1992).
[17] L. S. Bontuyan, A. G. Suits, P. L. Houston, and B. J. Whitaker, J. Phys. Chem. **97**, 6342 (1993).
[18] G. C. Neilson, G. A. Parker, and R. T Pack, J. Chem. Phys. **66**, 1396 (1977).
[19] (a) Z. T. Alwahabi, C. G. Harkin, A. J. McCaffery, and B. J. Whitaker, J. Chem. Soc. Faraday Trans. **85**, 1003 (1989); (b) A. J. McCaffery, Z. T. Alwahabi, M. A. Osborne, and B. J. Whitaker, J. Chem. Phys. **98**, 4586 (1993); (c) M. A. Osborne and A. J. McCaffery, *ibid*. **101**, 5604 (1994).
[20] A. J. Marks, J. Chem. Soc. Faraday Trans. **90**, 2857 (1994).
[21] (a) C. Atkins, D. Philos. thesis, Oxford, 1986; (b) R. Freeman and R. W. Nicholls, J. Mol. Spectrosc. **75**, 223 (1980).
[22] R. A. Copeland and F. F. Crim, J. Chem. Phys. **78**, 5551 (1983).
[23] (a) M. A. H. Smith, C. P. Rinsland, B. Fridovich, and K. N. Rao, in *Molecular Spectroscopy: Modern Research*, Vol. 3, edited by K. N. Rao (Academic, New York, 1985), p. 112; (b) A. S. Pine, A. G. Maki, and N.-Y. Chou, J. Mol. Spectrosc. **114**, 132 (1985); (c) A. S. Pine, J. Chem. Phys. **91**, 2002 (1989).
[24] I. R. Sims and I. W. M. Smith, Ann. Rev. Phys. Chem. **46**, 109 (1995).